Journal of Human Evolution 139 (2020) 102689

Contents lists available at ScienceDirect

Journal of Human Evolution

journal homepage: www.elsevier.com/locate/jhevol

A descriptive and comparative study of two Early Pleistocene immature scapulae from the TD6.2 level of the Gran Dolina cave site (Sierra de Atapuerca, Spain)

José María Bermúdez de Castro [a, b, *], Marina Martínez de Pinillos [a], Lucía López-Polín [c], Laura Martín-Francés [d, a], Cecilia García-Campos [a], Mario Modesto-Mata [e], Jordi Rosell [f, c], María Martinón-Torres [a, b]

[a] Centro Nacional de Investigación sobre la Evolución Humana (CENIEH), Paseo de la Sierra de Atapuerca 3, 09002 Burgos, Spain
[b] Anthropology Department, University College London, 14 Taviton Street, London WC1 H 0BW, UK
[c] IPHES, Institut Català de Paleoecologia Humana i Evolució Social, Unit Associated to CSIC, C/Marcel.lí Domingo s/n-Campus Sescelades URV (Edifici W3), 43007 Tarragona, Spain
[d] Univ. Bordeaux, CNRS, MCC, PACEA, UMR 5199, F-33615 Pessac Cedex, France
[e] Equipo Primeros Pobladores de Extremadura, Casa de la Cultura Rodríguez Moñino, Avda. Cervantes s/n., 10003 Cáceres, Spain
[f] Área de Prehistoria, Universitat Rovira i Virgili (URV), Avinguda de Catalunya 35, 43002 Tarragona, Spain

ARTICLE INFO

Article history:
Received 21 March 2019
Accepted 9 October 2019
Available online xxx

Keywords:
Pleistocene
Human evolution
Europe
Sierra de Atapuerca
Gran Dolina
Scapulae

ABSTRACT

Here we present the descriptive and comparative study of two immature scapulae recovered from the TD6.2 level of the Gran Dolina cave site (Sierra de Atapuerca, Spain) and assigned to *Homo antecessor*. This is the first time that data on the morphology and dimensions of the scapulae of a European late Early Pleistocene hominin population are provided. Considering the state of development and the linear dimensions, the scapula ATD6-116 could belong to a child of about 2–4 years. The morphology of ATD6-116 clearly departs from that of the *Australopithecus afarensis* juvenile specimen DIK-1-1, pointing to functional differences in locomotor behavior between *Australopithecus* and the late Early Pleistocene hominins. The immature scapula ATD6-118 belonged to an immature individual with a development of the scapula equivalent to that of adolescents of recent human populations. The scapulae ATD6-118 and KNM-WT 15000 present a similar state of development. Although the scapula KNM-WT 15000 is clearly larger than ATD6-118, these two specimens share some characteristics such as their relative narrowness and the value of the axilloglenoid and spinoglenoid angles. The glenoid fossa of ATD6-116 show a lateral orientation, whereas in ATD6-118 the glenoid fossa is slightly cranially oriented, but still within the range of variation of modern humans. The glenoid index of both ATD6-116 and ATD6-118 is low in accordance to the values usually observed in other early hominins, thus showing the primitive condition for this feature. Both scapulae show a ventrally placed axillary sulcus. The presence of this primitive feature in ATD-116 confirms that the shape of the axillary border has a genetic basis and it is not related to physical activity.

Published by Elsevier Ltd.

1. Introduction

The scapula is poorly represented in the hominin fossil record. The fragility of this bone, especially in immature individuals, is an important handicap to its preservation. In particular, the blade of the scapula, where muscles such as subscapularis, infraspinatus, and supraspinatus are attached, can be easily broken, even in recent populations. In this context, the discovery of Plio-Pleistocene specimens always represents an important advance for evolutionary studies and can shed light on issues such as past locomotor behaviors (Johanson et al., 1982; Alemseged et al., 2006; Haile-Selassie et al., 2010; Green and Alemseged, 2012; Churchill et al., 2018).

Comparative scapular morphology also is important to the fields of taxonomy and phylogeny, especially in the distinction between

* Corresponding author.
E-mail addresses: josemaria.bermudezdecastro@cenieh.es (J.M. Bermúdez de Castro), marinampg@hotmail.com (M. Martínez de Pinillos), lucia.lopezpolin@iphes.cat (L. López-Polín), lauramartinfrancesmf@gmail.com (L. Martín-Francés), cecilia.garcia@cenieh.es (C. García-Campos), paleomariomm@gmail.com (M. Modesto-Mata), jordi.rosell@urv.cat (J. Rosell), maria.martinon@cenieh.es (M. Martinón-Torres).

https://doi.org/10.1016/j.jhevol.2019.102689
0047-2484/Published by Elsevier Ltd.

Neandertals and modern populations (Endo and Kimura, 1970; Billy, 1975; Trinkaus, 1977, 1983, 2006, 2008; Churchill and Trinkaus, 1990; Churchill, 1996; Moran and Chamberlain, 1977; Carretero et al., 1997; Weaver, 2009; Trinkaus et al., 2016; Di Vincenzo et al., 2019). In particular, scapular axillary border morphology is one of the main postcranial features used to distinguish Neandertals from other hominins.

As noted above, the number of scapulae in the hominin fossil record of the Early Pleistocene is particularly poor. Apart from fragments of KNM-ER 1808 (Walker et al., 1982; Leakey and Walker, 1985), and D4166 from Dmanisi (Lordkipanidze et al., 2007), the complete right scapula of KNM-WT 15000 (Walker and Leakey, 1993), and the partial scapula KNM-ER 47000A (Green et al., 2018) we have no other available specimens. Here we present a description of two immature scapulae recovered during the 2005, 2006 and 2007 excavation seasons from level TD6.2 of the Gran Dolina site in the Sierra de Atapuerca Spain. ATD6-116 belonged to a child, who could be between 2 and 4 years old according to its state of development and the size standards of recent human populations, while ATD6-118 would have a development stage equivalent to that of current adolescents. These specimens, attributed to *Homo antecessor*, have not yet been published so this is the first time the morphology and metrics of this skeletal element in a European hominin species of the late Early Pleistocene has become available to the scientific community. Given the phylogenetic proximity of *H. antecessor* to other European Middle Pleistocene hominins (like the Sima de los Huesos specimens) and the Neanderthals, these specimens offer important new information with regard to these hominins. In addition, the TD6.2 specimens offer data about the morphology of the scapulae during the final stretch of human evolution. In this study we present a preliminary description and comparison of the specimens. A more detailed study about the growth and development of *H. antecessor* with respect to modern populations will be the object of a later study.

1.1. The Gran Dolina TD6.2 level

The TD6.2 level of the Gran Dolina cave site (Campaña et al., 2016 and references therein) has yielded about 170 human remains belonging to a minimum of eight individuals (Bermúdez de Castro et al., 2017). These remains are well preserved, though fragmented probably due to at least two cannibalism events (Fernández-Jalvo et al., 1999; Carbonell et al., 2010; Saladié et al., 2012). The human remains, as well as more than 831 lithic artifacts (Mosquera et al., 2018) and several thousand fossil remains of different species of micro and macrovertebrates, were obtained during two different periods, 1994–1996 and 2003–2007 (Carbonell et al., 1995; Bermúdez de Castro et al., 2008).

A combination of different dating methods indicates an age range of 0.8–0.9 Ma (Falguères et al., 1999; Berger et al., 2008; Arnold et al., 2014; Arnold and Demuro, 2015; Moreno et al., 2015; Duval et al., 2018). Parés and Pérez-González (1995, 1999) observed a polarity reversal between TD7 and TD8, interpreted as the Matuyama/Brunhes boundary, meaning that levels TD8 to TD11 were deposited during the Middle Pleistocene, whereas levels TD1 to TD7 were deposited during the Early Pleistocene (see also a recent study by Álvarez-Posada et al., 2018). Finally, a recent paleomagnetic study of the interior facies of TD1 place the TD6.2 hominins between the Matuyama/Brunhes boundary and the Jaramillo subchron (Parés et al., 2018). Considering these studies together, and taking into account the biostratigraphic information from TD6 (Cuenca-Bescós et al., 2015), we suggest that the TD6 hominins should be assigned to the Marine Isotope Stage 21 (MIS 21).

2. Materials and methods

2.1. The TD6.2 scapulae

The two scapulae recovered from the TD6.2 level of the Gran Dolina cave site belonged to immature individuals. The right ATD6-116 scapula was recovered in 2005 in square G14, whereas the right ATD6-118 scapula was recovered in two different years (2006 and 2007) in square F12 (see the map of the excavation in Bermúdez de Castro et al., 2008).

2.2. Restoration and preservation

ATD6-116 (Fig. 1) was recovered in a block adhered to the hardened clay of the site and restored over several months by L. López-Polín at the Restoration Laboratory of the IPHES, in Tarragona, Spain. Although the scapular body was fragmented, the digital reconstruction of most of the specimen, which still remains in the matrix block, was possible [Supplementary Online Material (SOM), Figs. S1, S3, S4, and S5]. Numerous cracks revealed postmortem fractures of the blade and other portions of the specimen. Most of the fractures occurred during the excavation due to the fragility of the bone and the hardness of the sediment. However, the specimen is very well-preserved.

ATD6-118 (Figs. 2 and 3) was also restored from different fragments (SOM 1, Figs. S2, S6, and S7). Some parallel and long cutmarks are present in the subscapular fossa, as well as three short, parallel ones at the level of the infraglenoid tuberosity, where the long head of the triceps brachialis attaches. These marks are probably related to the cannibalism events inferred from the taphonomic studies carried out on the TD6.2 hominin sample (Fernández-Jalvo et al., 1999; Carbonell et al., 2010; Saladié et al., 2012). ATD6-118 lacks the acromion epiphysis and the coracoid process. However, some portion of the subcoracoid center was in process of ossification. Several parts of the scapula, including the superior and inferior borders, the upper part of the vertebral border, and the spine are damaged. Despite this damage, most measurements can be obtained with reasonably accuracy.

2.3. Methods

Both scapulae were scanned using the Phoenix v/tome/x s (GE Measurement & Control) housed at the National Research Center on Human Evolution (CENIEH, Burgos, Spain). The scans were performed with a 0.2 mm Copper filter, 160 kV, 450 μA and voxel size of 55 μm for ATD6-116, and a 130 kV, 400 μA and voxel size of 86 μm for ATD6-118. ATD6-116 was digitally extracted from the matrix. The final volumes were reconstructed using Amira 6.7.0 software (Visage Imaging, Inc.). The scapulae were semi-automatically segmented, with manual editing and a non-local mean filter.

Following Frutos (2002), Odwak (2006), Rissech and Black (2007), and Dabbs and Moore-Jansen (2010) we obtained from the digital images seven linear measurements (maximum scapular length (MSL), scapular breadth (SB), supraspinous breadth (SSB), infraspinous breadth (ISB), glenoid fossa height (GH), glenoid fossa breadth (GB), and axillary border thickness (ABT) (Table 1), as well as three angles (axilloglenoid angle (A/G), axillospinal angle (A/S), and spinoglenoid angle (S/G) (Table 1 and Fig. 4). Four standard indices (scapular index, supra-infra scapular index, glenoid index, glenoid size) were generated from the linear dimensions (Table 1).

For comparative purposes we employed the cast of KNM-WT 15000, and the rest of measurements were extracted from the literature (Eickstedt, 1925; Vallois, 1928–1946; Senut, 1981; Johanson et al., 1982; Carretero et al., 1997; Trinkaus, 2006, 2008;

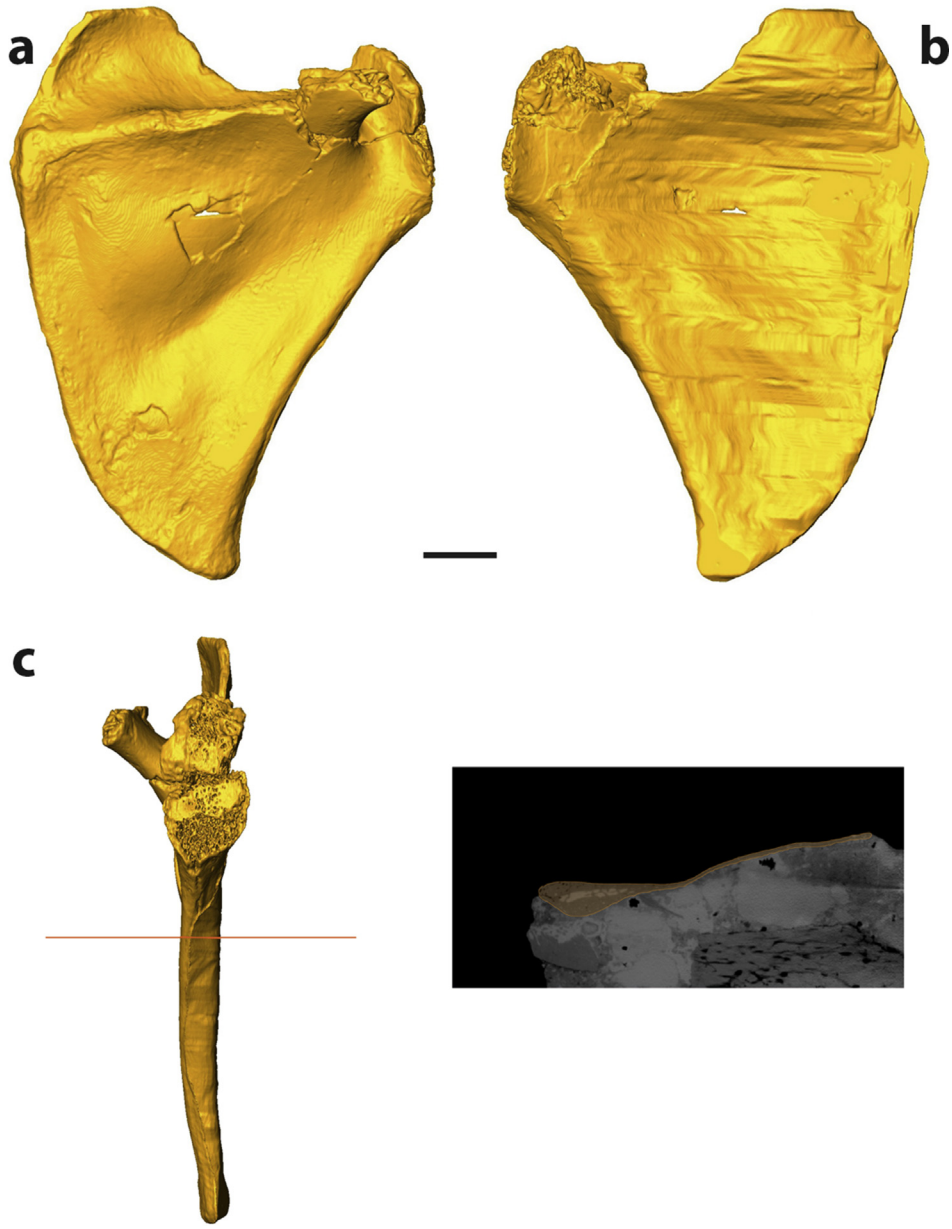

Figure 1. Digital images of the ATD6-116 scapula. a) dorsal view; b) ventral view; c) laterocaudal view (yellow silhouette) and cross section below the infraglenoid tubercle. The section is orientated mediolaterally, with the dorsal surface above. Scale bar = 2 cm. (For interpretation of the references to color in this figure legend, the reader is referred to the Web version of this article.)

Alemseged et al., 2006; Lordkipanidze et al., 2007; Berger et al., 2010; Haile-Selassie et al., 2010; Green and Alemseged, 2012; Badr El Dine and Hassan, 2016; Feuerriegel et al., 2017; Churchill et al., 2018; Di Vincenzo et al., 2019). Despite the sparse fossil record, it is still possible to track the evolution of the main features (angles and dimensions of the glenoid fossa) throughout human evolution.

3. Results

3.1. Age at death and sex

Since we are dealing with a population from the late Early Pleistocene, it is not possible to accurately assign the age of death for ATD6-116 and ATD6-118 using present human population patterns. That is, we do not know if the European Early Pleistocene populations exhibited a long adolescence period, like in modern humans, or even the duration of the childhood period (Modesto-Mata, 2019). We have some information suggesting that the stature of the TD6.2 hominins could be similar to that of some recent populations (Carretero et al., 1999), but this does not inform us about the rate of growth of *H. antecessor*. We can compare scapular dimensions to those of modern populations, but such comparisons are limited by the fact that *H. antecessor* could have had an accelerated development as compared to *Homo sapiens* (Modesto-Mata, 2019). In the case of the scapula ATD6-116, if we consider the dimensions obtained by Badr El Dine and Hassan (2016) in a recent Egyptian population, the maximum scapular length obtained in this specimen (Table 2) would correspond to a child ranging in age from 2 to <4 years (95% confidence for the mean value of this age interval).

On the other hand, the specimens ATD6-118 and KNM-WT 15000 show a similar degree of development, equivalent to that of modern human adolescents (Fig. 5). Using modern human

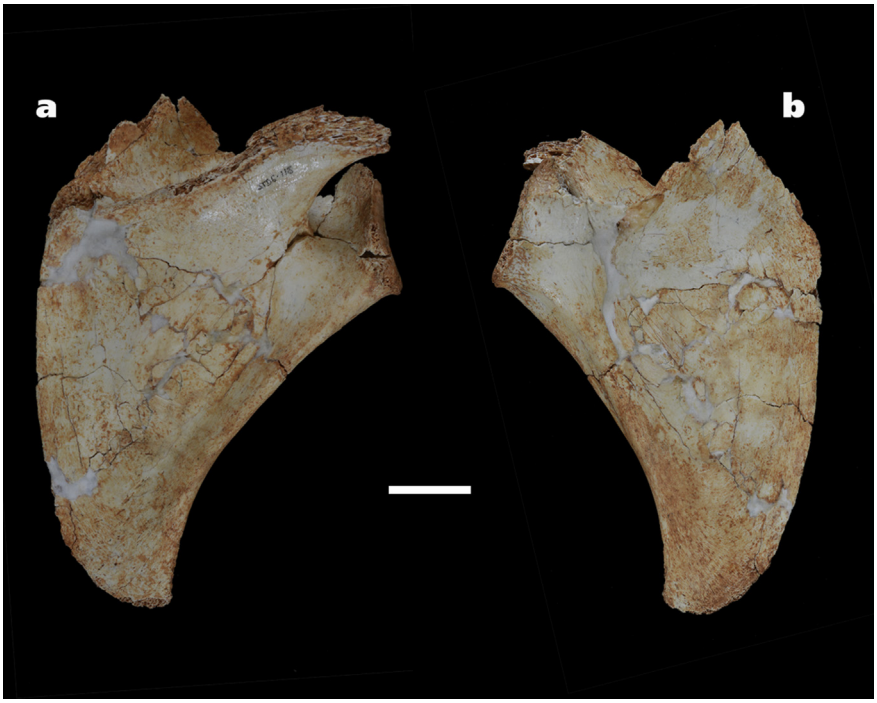

Figure 2. Photographs of the ATD6-118 scapula. a) dorsal view; b) ventral view; Scale bar = 1 cm.

standards, and assuming that the skeleton KNM-WT 15000 is male (Brown et al., 1985), the age of death of this individual was about 11 years according to his dental age, and 13–13.5 years according to his skeletal age (Smith, 1993). However, the dental histological study of this specimen suggests an age at death closer to 8 or 9 years (Dean et al., 2001; Dean, 2007) suggesting that his skeletal age was also less than 13.0–13.5 years. Given the similarity between ATD6-118 and KNM-WT 15000 we can make a first guess that the ATD6-118 specimen was less than 13 years old when it died. Unfortunately, ATD6-118 is not associated with any dental remains (Bermúdez de Castro et al., 2017). Furthermore, given the temporal separation between KNM-WT 15000 and ATD6-118 (about 0.8 Ma), we cannot know if the dental and skeletal development of KNM-WT 15000 and *H. antecessor* were similar.

Using radiographic images from two large samples of modern humans, Schaefer et al. (2015) conclude that modern humans (both males and females) who lack the acromial apophysis are likely to be under the age of 15–16 years. Despite the deterioration suffered by ATD6-118 it is clear that the subcoracoid secondary center is present, but incompletely fused. By this standard, if ATD6-118 belonged to a modern population, it would be younger than 14–15 years old (Scheuer and Black, 2004; Di Vincenzo et al., 2012). In contrast, the maximum scapular length of ATD6-118 (Table 2) corresponds to the mean measurements obtained by Badr El Dine and Hassan (2016) in individuals from 16 to <22 years. Therefore, since we do not know the pattern of growth and development of *H. antecessor*, a conservative estimate of the developmental age of ATD6-118 is that it belonged to an immature individual with scapular development equivalent to that of recent human adolescents.

With respect to sex, the data are insufficient for sex determination of ATD6-116 and ATD6-118.

3.2. Measurements and indices

Table 2 presents the values for ATD6-116 and ATD6-118 of the different measurements and indices. Regarding early hominins, we can only compare ATD6-116 with the Dikika specimen (DIK-1-1), attributed to *Australopithecus afarensis*, which could have had an approximately similar age at death (Alemseged et al., 2006). However, the supra- and infraspinous breadths clearly differentiate ATD6-116 and DIK-1-1 (Table 2). Bivariate regression of the ln-transformed dimensions places ATD6-116 near the regression line of *H. sapiens*, whereas DIK-1-1, which possess a relatively longer suprascapular breadth, falls between the regression lines of *H. sapiens* and those of the great apes (see S6e of the supplementary information of Alemseged et al., 2006). Furthermore, the value of the infrascapular breadth/glenoid size in ATD6-116 is 3.8, clearly higher than that of the DIK-1-1 and within the range of variation of *H. sapiens* (Green and Alemseged, 2012).

Although ATD6-118 is an immature specimen it is possible to draw some rough conclusions about its general dimensions. In their study of scapulae of an Egyptian population, Badr El Dine and Hassan (2016) note that the value of the scapular index is fixed from a very early age, around 4 years. The value of this index in ATD6-118 (65.1) is among the lowest values compared to a modern sample of 126 scapulae from North India (mean value: 73.3; SD = 4.8; range: 62.5–89.6) studied by Chhabra et al. (2015). KNM-WT 15000, which seems to be at a similar developmental stage as ATD6-118, has a considerably higher maximum scapular length and scapular breadth (Table 2). However, the scapular index of KNM-WT 15000 is also low (62.2). Therefore, it seems that the Early Pleistocene scapulae are relatively narrower compared to those of modern humans. Although these data are not conclusive, given the limitations of the fossil sample ($n = 2$), it can be hypothesized that the scapulae of the hominins of the Early Pleistocene could be relatively narrower than those of modern human populations.

The supra-infra scapular index reflects the proportion between the supraspinous and infraspinous breadth. For ATD6-116 the value of this index is 34.2 as a result of its transversely oriented scapular spine. This value is less than half that of the value obtained for the DIK-1-1 specimen (Green and Alemseged, 2012), which exhibits an obliquely oriented spina. Figure 6 shows the scatterplot of the log supraspinous breadth vs. log infraspinous breadth of DIK-1-1,

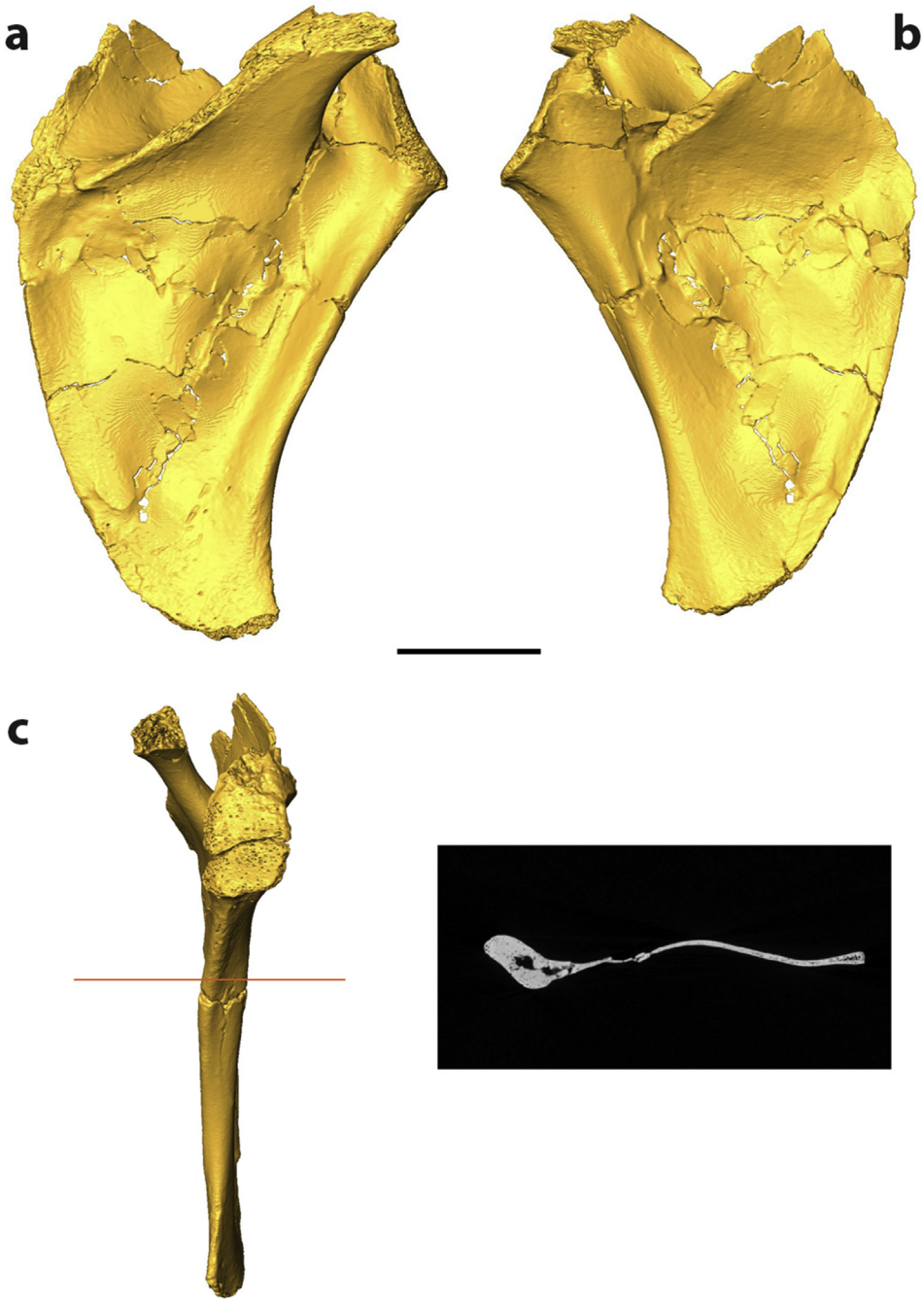

Figure 3. Digital images of the ATD6-118 scapula. a) dorsal view; b) ventral view; c) laterocaudal view and cross section. Scale bar = 3 cm.

ATD6-116, and three hominin samples. Note that ATD6-116 aligns with the sample of *H. sapiens*. In ATD6-118 the scapular spine is almost transversely oriented and the value of the supra-infra scapular index is somewhat larger (46.4) than in ATD6-116. This figure is clearly lower than the figure (55.4) obtained by Churchill et al. (2018) in MH2, and similar to the mean value reported by these authors for adults of a recent modern human sample (X = 44.0; S.D = 5.0; n = 47).

The height of the glenoid fossa in ATD6-118 is only a little smaller than the mean values for adult Neanderthals, Atapuerca-SH hominins, and the fossil and anatomically modern humans (Churchill and Trinkaus, 1990; Carretero et al., 1997; Badr El Dine and Hassan, 2016; Di Vincenzo et al., 2019) (Table 3). The glenoid fossa of the small scapula A.L. 288-1l has a height of 27.0 mm, whereas the values of Sts 7 (38.0) and KNM-WT 15000 (33.7) are not very different from that of ATD6-118 (Carretero et al., 1997). In contrast, the breadth of the glenoid fossa of ATD6-118 is less than the mean values of the adult Atapuerca-SH hominins, Neanderthals, and the fossil and anatomically modern humans (Carretero et al., 1997; Di Vincenzo et al., 2019). Even the breadth of the glenoid fossa of Sts 7 (22.4) and KNM-WT 15000 (20.2) are greater than that of ATD6-118 (Table 3). Figure 7 shows the scatterplot of the glenoid fossa height (GH) vs. the glenoid index (GI) in some fossil and recent humans. The values of ATD6-116 and ATD6-118 are far from the variability of *H. neanderthalensis* and *H. sapiens*.

Table 1
Linear measurements,[a] standard indices generated from these linear measurements, and the angles obtained in the scapulae ATD6-116 and ATD6-118.

Variable	Abbreviation	Definition
Maximum scapular length (height)	MSL	The maximum distance between the highest point of the superior angle and the lowest point of the inferior angle.
Scapular breadth (width)	SB	The distance between the middle of the dorsal border of the glenoid fossa to the end of the spinal axis on the vertebral border.
Supraspinous breadth	SSB	The distance between the point at which the axis of the spine meets the medial border of the scapula to the superior angle.
Infraspinous breadth	ISB	The distance between the point at which the axis of the spine meets the medial border of the scapula to the inferior angle.
Glenoid fossa height	GH	The maximum distance from the superior margin of the glenoid fossa to the inferior margin of this fossa.
Glenoid fossa breadth	GB	The maximum distance across glenoid fossa measured perpendicular to the axis of glenoid fossa height.
Axillary border thickness	ABT	The antero-posterior maximum thickness of the lateral margin just inferior to the infraglenoid tubercle.
Scapular index	SB/MSL = SI	The percentage ratio between scapular breadth and the scapular length.
Supra-infra scapular index	SSB/ISB = SSI	The percentage ratio between the supraspinous and infraspinous lengths.
Glenoid index	GB/GH = GI	The percentage ratio between the glenoid fossa breadth and the glenoid fossa height.
Glenoid size		The square root of the product of glenoid height and breadth (Churchill et al., 2018).
Axilloglenoid angle	A/G	The angle formed by the axillary border and the glenoid height line.[b] This angle is a measure of the glenoid fossa orientation.
Axillospinal angle	A/S	The angle formed by the axillary border and the base of the spine.[c]
Spinoglenoid angle	S/G	The angle formed by the base of the spine and the glenoid height line.[c] This angle is also a measure of the glenoid fossa orientation.

[a] The linear measurements are in millimetres and were obtained from the digital images.
[b] We have taken the angle according to the methodology of Martin (1928) and Robinson (1972). See a detailed description of this measurement in Figure 4 of this report and in Figure 4 of Di Vincenzo et al. (2019).
[c] Following Martin (1928), and see Di Vincenzo et al. (2019).

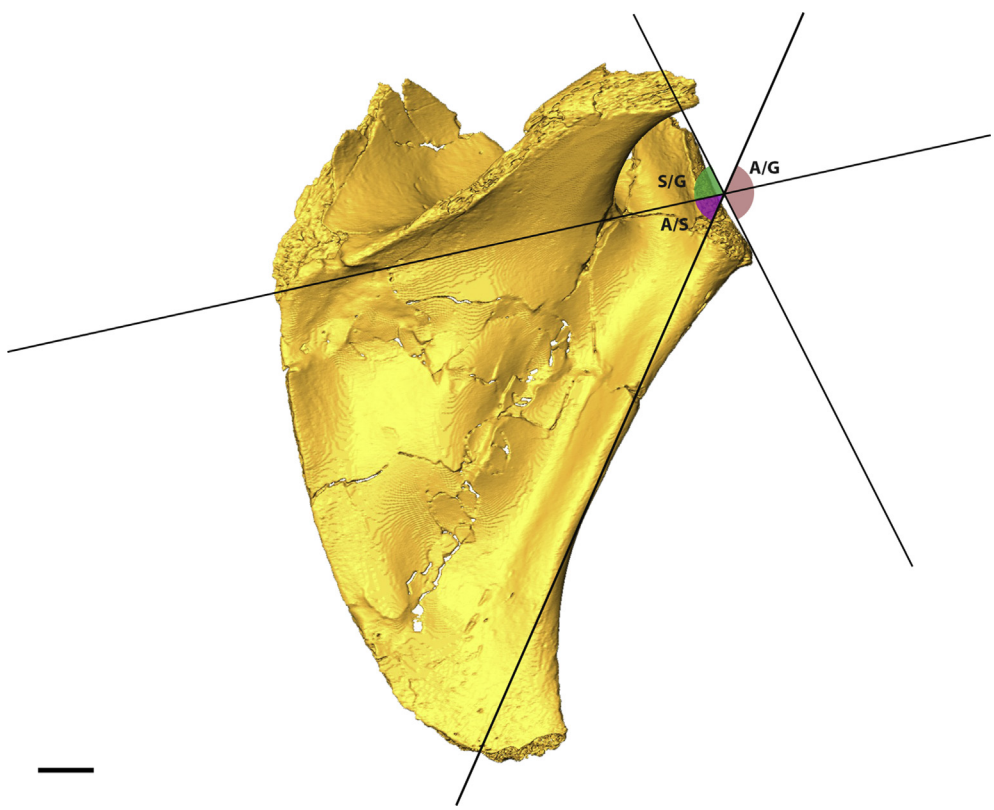

Figure 4. Digital image of ATD-118, showing the angles obtained in both ATD6-116 and ATD6-118. A/G: Axilloglenoid; A/S: Axillospinal angle; S/G: Spinoglenoid angle. Scale bar = 1 cm.

The axilloglenoid angle of ATD6-116 (143°) is clearly higher than that of DIK-1-1 (Green and Alemseged, 2012) (Tables 2 and 4). The axillospinal angle is also lower in DIK-1-1 (37°) than in ATD6-116 (58°). Finally, the spinoglenoid angle measures 82.9° in DIK-1-1, and 85° in ATD-116. The axilloglenoid angle of ATD6-118 is similar to that of KNM-WT 15000, KSD-VP-1/1 (Haile-Selassie et al., 2010; Churchill et al., 2018) and the mean value of the modern human sample quoted by Carretero et al. (1997) (Table 4), and clearly greater that those of MH2 (Berger et al. (2010) and Sts 7 (Green and Alemseged, 2012). However, the axilloglenoid angle of ATD6-118 is below the range of variation of the Atapuerca-SH hominins, European Neanderthals, and the Altamura specimen (Vallois, 1928–1946; Trinkaus, 1983; Green and Alemseged, 2012; Di Vincenzo et al., 2019) (Table 4).

Table 2
Measurements, indices, and angles of the scapulae ATD6-116, ATD6-118, DIK-1-1 (Dikika), and KNM-WT 15000.

	MSL[a]	SB	SI	SSB	ISB	SSI	GH	GB	GI	ABT	A/G	A/S	S/G
ATD6-116	81.2	56.0	68.9	22.5	65.8	34.2	24.4	11.9	48.8	5.6	143	58	85
ATD6-118	126.8	82.5	65.1	44.4	95.6	46.4	33.4	17.6	52.7	10.9	129	54	76
DIK-1-1 Right[b]	59.8	50.0	83.6	37.9	28.3	74.7	–	–	–	–	120	37.0	82.9
KNM-WT 15000	152.6	91.9	62.2	46.1	124.3	37.1	33.7	20.4	60.5	–	131.0	64.0	67.0

[a] Abbreviations: MSL: maximum scapular length; SB: scapular breadth; SI: scapular index; SSB: supraspinous breadth; ISB: infraspinous breadth; SSI: supra-infra-scapular index; GH: glenoid fossa height; GB: glenoid fossa breadth; GI: glenoid index; ABT: axillary border thickness; A/G: axilloglenoid angle; A/S: axillospinal angle; S/G: spino glenoid angle.
[b] Data of the DIK-1-1 specimens are from Green and Alemseged (2012).

Figure 5. Comparison between KNM-WT 15000 and ATD6-118. Both scapulae show a similar state of development. Note the difference in size between both specimens. Scale bar = 2 cm.

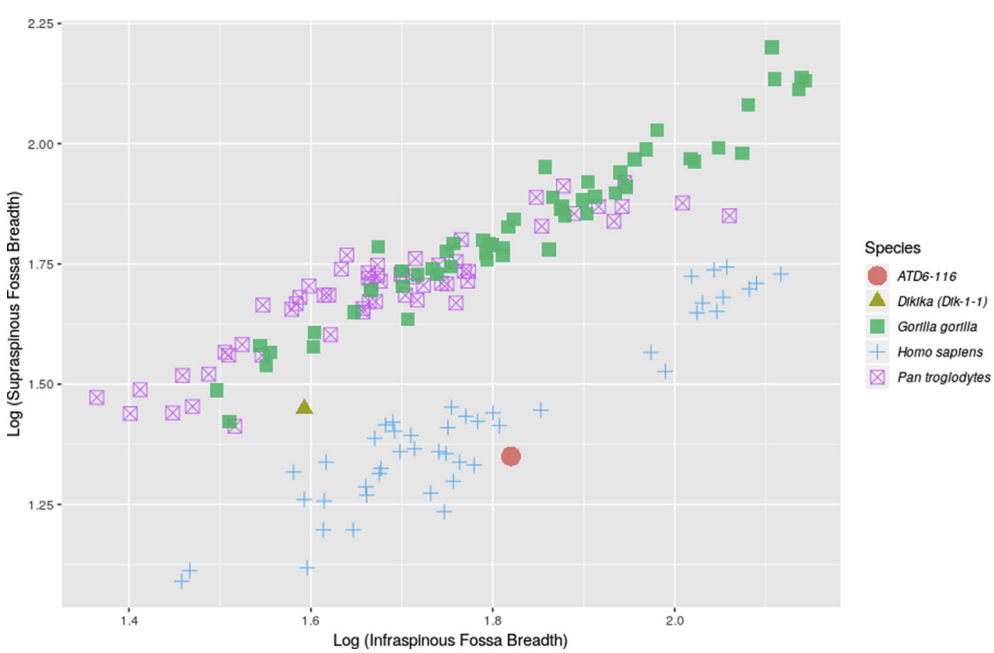

Figure 6. Scatterplot showing the distribution of the log supraspinous breadth vs. log infraspinous breadth of DIK-1-1, ATD6-116, and three hominin samples. This figure is based in figure S6e of Alemseged et al. (2006). Note that these authors use the terms supraspinous fossa breadth and infraspinous fossa breadth.

Table 3
Measurements of the glenoid fossa in some specimens and hominin samples.

Specimen/sample	GH[a]	GB	GI	Authors
ATD6-116	24.4	11.9	48.8	Authors
ATD6-118	33.4	17.6	52.7	Authors
A.L. 288-1l	27.0	18.1	67.0	Carretero et al. (1997)
Sts 7	38.0	22.4	58.9	Carretero et al. (1997)
KNM-WT 15000	33.7	20.4	60.5	Authors
AT-320	36.0	(23)[b]	63.8	Carretero et al. (1997)
AT-343	(37.0)	(23.0)	62.2	Carretero et al. (1997)
AT-794	40.0	26.8	67.0	Carretero et al. (1997)
Scapula 1 from Sima de los Huesos	(40.0)	(25.0)	62.5	Carretero et al. (1997)
Altamura	36.0	25.1	69.7	Di Vincenzo et al. (2019)
Neanderthals $n = 12$	37.0 ± 4.7	24.5 ± 3.7	66.0 ± 3.0	Carretero et al. (1997)
Fossil *H. sapiens* $N = 45$	36.0 ± 2.6	25.7 ± 2.1	71.32 ± 3.3	Di Vincenzo et al. (2019)
Coimbra. (modern humans) $N = 158$)	35.6 ± 3.3	25.8 ± 2.6	72.6 ± 4.2	Carretero et al. (1997)

[a] Abbreviations: GH: glenoid fossa height; GB: glenoid fossa breadth; GI: glenoid index.
[b] Parenthesis ( ) indicate estimated values.

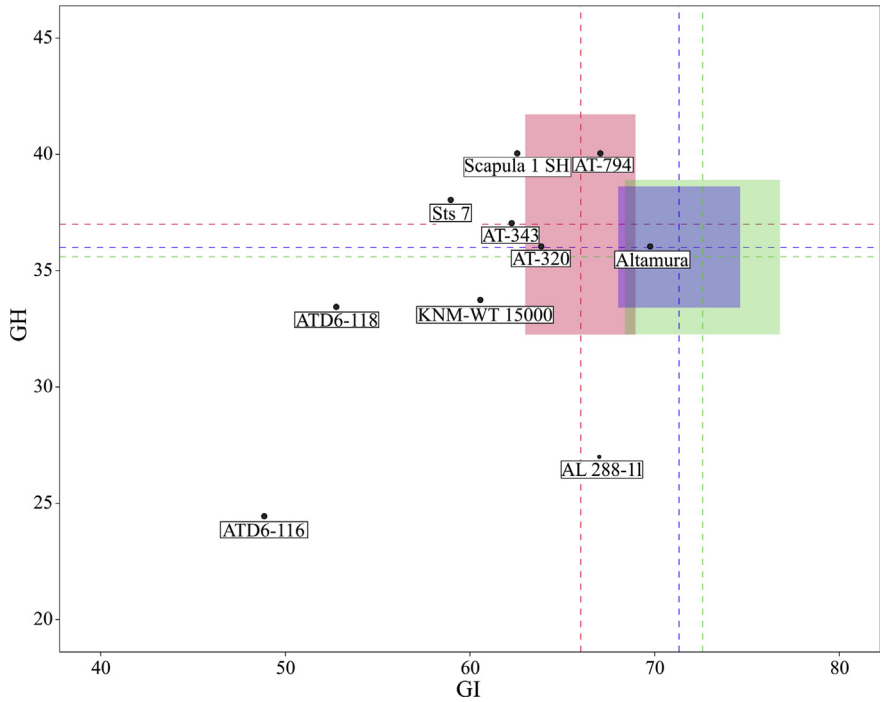

Figure 7. Scatterplot of the glenoid fossa height (GH) vs. the glenoid index (GI) in some fossil and recent humans. Dashed lines intersect in the average values of Neanderthals (pink), fossil *H. sapiens* (blue), and recent *H. sapiens* (green). The rectangles indicate the distribution area. See the data in Table 3. (For interpretation of the references to color in this figure legend, the reader is referred to the Web version of this article.)

The axillospinal angle in ATD6-116 and ATD6-118 is similar to those of Neanderthals and the Altamura specimen (Table 4), but below the range of anatomically modern humans (Table 4) and it is clearly lower than those of the Pliocene and Early Pleistocene fossils with the exception of KNM-WT 15000 (Tables 2 and 4). Regarding the spinoglenoid angle, the value of ATD6-116 is similar to those of other hominins, including Neanderthals and modern humans (Table 4). The value of this angle in ATD6-118, however, is below the range of variation of Neanderthals and modern humans and lower than all the specimens included in Table 4, again except for KNM-WT 15000.

3.3. Morphology

The most striking feature of the TD6.2 scapulae are their axillary borders. First, we note that both ATD6-116 and ATD6-118 exhibit an arced axillary border. It is particularly remarkable in ATD6-118. If we draw a straight line between the lower-most point of the glenoid fossa and the lower-most point of the axillary border, the maximum perpendicular distance between that straight line and arc of the axillary border is located approximately 58 mm from the inferior-most point of the glenoid fossa and measures 11.2 mm. In ATD6-116 the axillary border is also arced, but the arc is only well developed near the inferior angle. To the best our knowledge, the only fossil scapulae showing a marked arced axillary border are KNM-WT 15000 and KNM-ER 1808 (Walker and Leakey, 1993). The axillary border thickness of ATD6-118 is similar to that of the Altamura and Tabun C1 specimens, and clearly lower than in Kebara 2 and Neandertal 1 specimens (Di Vincenzo et al., 2019). The digital image of ATD6-118 shows a well-differentiated ventral bar.

Both ATD6-116 and ATD6-118 exhibit a dorsally placed axillary margin and a ventrally placed axillary sulcus (Figs. 1 and 3) (or a

Table 4
Values of the axilloglenoid angle (A/G), axillospinal angle (A/S), and spinoglenoid angle (S/G) in some fossil specimens and samples.

Specimen/sample	A/G	A/S	S/G	Authors
ATD6-116	143.0	58.0	85 .0	Authors
ATD6-118	129.0	54.0	76.0	Authors
DIK-1-1 (right side)	120	37.0	82.9	Green and Alemseged (2012)
KSD-VP-1/1	128.0	43.8	80.6	Haile-Selassie et al. (2010) and Churchill et al. (2018)
KNM-ER 47000 A	–	29.1	90.9	Churchill et al. (2018)
A.L. 288 1l	–	38.2	83.7	Churchill et al. (2018)
MH2	114.0	40.0	83.5	Berger et al. (2010)
Sts 7	116.0	29.8	83.4	Green and Alemseged (2012)
U.W. 101-1301	–	26.8	–	Feuerriegel et al. (2017)
KNM-WT 15000	131.0	64.0	67.0	Authors
AT-320 (Sima de los Huesos)	140.0	–	–	Carretero et al. (1997)
AT-801	144.0	–	89.0	Carretero et al. (1997)
Scapula I from Sima de los Huesos	–	–	87.0	Carretero et al. (1997)
Altamura	143.5	58.0	85.0	Di Vinzenzo et al. (2019)
European Neanderthals	140.6 ± 5.3; $n = 9$ (132–150)	56.7 ± 1.5; $n = 6$	84.7 ± 5.0; $n = 6$ (77.0–93.0)	Carretero et al. (1997)
Skhul 4	–	52.0	–	Di Vinzenzo et al. (2019)
Skhul 5	–	51.0	–	Di Vinzenzo et al. (2019)
Modern humans	132.0 ± 5.2 (119.5–140.1)	42.7 ± 2.7 (34.6–47.8)	89.1 ± 4.4	Carretero et al. (1997)

sulcus axillaris subscapularis, in the terminology of Eickstedt [1925]). This is the predominant condition in modern humans, and different from the pattern found in the Atapuerca-SH hominins and Neanderthals (Carretero et al., 1997; Trinkaus, 2006, 2008). Many of the Neanderthals possess an axillary sulcus dorsally placed, the so-called sulcus axillary teretis (sensu Eickstedt, 1925), and an associated ventrally placed axillary margin (Table 5). *Australopithecus* (Sts 7, Stw 431, A.L. 288-1l, and KSD-VP-1/1), and early *Homo* (KNM-WT 15000 and Dmanisi 4166) show a ventral sulcus (Senut, 1981; Johanson et al., 1982; Walker and Leakey, 1993; Lordkipanidze et al., 2007; Melillo, 2016). All Atapuerca-SH scapulae exhibit a dorsal sulcus (Carretero et al., 1997), whereas there is a noticeable variability in Neanderthals and early *H. sapiens* (Trinkaus, 1977, 2006; 2008). Early *H. sapiens* (e.g., Skhul and Qafzeh and other late Pleistocene hominins) and recent modern populations tend to have either a ventral sulcus or one of intermediate morphology, the so-called bisulcate pattern. This pattern is characterized by a crest placed in the middle of the axillary border, small sulci adjacent to the crest, and convex dorsal and ventral surfaces (Vallois, 1928–1946; Endo and Kimura, 1970; Trinkaus, 1977, 2006, 2008 Churchill, 1996). The ventral sulcus is rare in Neanderthals, but the three patterns are present in anatomically modern humans (Carretero et al., 1997; Voisin, 2011). It is also interesting to note that, according to Churchill (1994), this qualitative classification does not reflect the continuous variation of this region of the scapula. Trinkaus (2008, Table 5) also had problems categorizing the morphology of axillary border of the Krapina scapulae.

In ventral view, a small scapular notch is seen in the superior border of ATD6-116. The scapular notch cannot be detected in the reconstructed superior border of ATD6-118.

4. Discussion

The scapula is a skeletal element poorly represented in the fossil record, with few complete specimens (e.g., Brown et al., 1985; Alemseged et al., 2006). Most of the specimens are fragmented yielding only partial morphological information. Despite this, there is a great deal of interest concerning taxonomic and functional inferences that can be made from the study of the scapula (e.g., Trinkaus, 1977; Churchill and Trinkaus, 1990; Haile-Selassie et al., 2010; Green and Alemseged, 2012; Macias and Churchill, 2015; Feuerriegel et al., 2017). The TD6.2 level from the Gran Dolina site (Sierra de Atapuerca) has yielded two almost complete immature scapulae. These specimens, together with the scapula D4166 from Dmanisi, are the only ones represented so far in the Early Pleistocene of Eurasia providing an excellent opportunity to learn about the scapula of the genus *Homo* in this period. Although the age at death of the immature individuals ATD6-116 and ATD6-118 is

Table 5
Comparative frequencies of axillary border morphology in some specimens and samples.

Specimen/sample	Dorsal	Bisulcate	Ventral	Authors
ATD6-116			X	Authors
ATD6-118			X	Authors
Sts 7			X	Senut (1981)
Stw 431			X	Senut (1981)
A.L. 288-1l			X	Johanson et al. (1982)
KNM-WT 15000			X	Authors
Dmanisi D4166			X	Lordkipanidze et al. (2007)
Altamura AB (1–3)			X	Di Vincenzo et al. (2019)
ATA-SH, $n = 4$	100%	–	–	Carretero et al. (1997)
Neanderthals, $n = 25$	72.0%	28.0%	–	Carretero et al. (1997)
Krapina, $N = 15$	60.0%	36.7%	3.3%	Trinkaus (2006)
Skhul/Qafzeh, $n = 4$	–	100%	–	Carretero et al. (1997)
Coimbra, modern humans, $n = 248$	–	32.7%	67.3%	Carretero et al. (1997)
Europeans/Austria	1.0%	13.4%	85.6%	Eickstedt (1925)

uncertain, the information they provide about scapular morphology is clearly very valuable.

The qualitative morphology and metric dimensions of ATD6-116 are similar to those of modern humans, and clearly differ from the juvenile specimen of *A. afarensis* DIK-1-1. For instance, the high supra-infra scapular index in DIK-1-1 (74.7 right side) is a consequence of an obliquely oriented scapular spine, which produces an exaggerated supraspinous breadth relative to the infraspinous breadth comparable to suspensory great apes (Green and Alemseged, 2012). The oblique orientation of the spine in specimens such as DIK-1-1 and MH2 may well reflect the locomotor behavior of *Australopithecus*, which is thought to include a substantial amount of climbing (Green and Alemseged, 2012; Churchill et al., 2018). In contrast, the transverse orientation of the spine in the TD6.2 scapulae is in accordance with bipedalism and the loss of the climbing abilities during the evolution of the genus *Homo*.

In their comparative study of the DIK-1-1 scapula Green and Alemseged (2012) note that the cranial orientation of the glenoid fossa, a feature which can be evaluated with the axilloglenoid angle, remains relatively stable during ontogeny in both *Australopithecus* and great apes and it is thus not dependent on size. The adult specimens A.L. 288-1l, Sts 7, and KSD/-VP-1/1 show a similar cranially oriented shoulder joint to that observed in DIK-1-1, suggesting arboreal adaptations of these early hominins. In ATD6-116 the value of the axilloglenoid angle is remarkable (143°), whereas in ATD6-118 the value of this angle is 129°, similar to the values obtained in KSD-VP-1/1 (Haile-Selassie et al., 2010), and KNM-WT 15000. It is important to remember that the value of the axilloglenoid angle varies according to the method used. For example, the differences between the results obtained in Sts 7 by Vrba (1979), Senut (1981), and Green and Alemseged (2012) are remarkable. The value measured by the last authors for KNM-WT 15000 is 137.8, a figure different to that we have obtained and that reported by Carretero et al. (1997). Despite these concerns, though, the trend observed in the literature shows low values for this angle in early hominins, close to the range of variation of the great apes. In contrast, the range of variation of recent modern humans includes values similar to that of ATD6-118 (Carretero et al., 1997; Churchill et al., 2018).

The average of the glenoid index in modern populations is statistically significantly higher than that of Neanderthals (Vallois, 1928–1946; Endo and Kimura, 1970; Trinkaus, 1983; Churchill and Trinkaus, 1990; Carretero et al., 1997). We have verified that the glenoid index is also low in other ancient hominins (Sts 7, KNM-WT 15000), as noted by Robinson (1972), Vrba (1979), and Senut (1981). In the case of the *H. antecessor* scapulae, the figures obtained may be influenced by the state of preservation and the lack of complete ossification of the glenoid fossa. Regardless, the values of the glenoid index in ATD6-116 and ATD6-118 are clearly below the range of variation of fossil hominins (Table 3). It is interesting to note that Badr El Dine and Hassan (2016) found that this index is not dependent of the age, at least in modern humans.

The glenoid index is influenced by the shape of the glenoid fossa. Modern humans tend to have glenoid fossae that are relatively broad in an anterior-posterior direction, with a more laterally projecting anterior margin of the joint surface, whereas the glenoid fossa in Neanderthals tends to be elongated in a superior-inferior direction and narrow in an anterior-posterior direction. Di Vincenzo et al. (2012, p. 282) suggest that "the main differences in the shape of the glenoid fossa (SGF) morphology among and between species in the genus *Homo* are related to differing degrees of development of its different components". In particular, the inferior shoe-shaped center of ossification forms three fourths of the glenoid and defines the maximum breadth of this surface in the adult. The differential growth rates would result in a progressive dorso-ventral expansion of the glenoid fossa, which would be the derived condition in relation to the narrow, primitive condition in early hominins. A recent study by Macias and Churchill (2015) discusses the evolutionary-developmental hypothesis posed by Di Vincenzo et al. (2012) to explain the relatively broad glenoid in anatomically modern humans, since we share this feature with chimpanzees. According to Macias and Churchill (2015), chimpanzees and modern humans would have different developmental processes to achieve a similar (convergent) morphology. These authors suggest that changes in the morphology of the glenoid fossa across human evolution may reflect an evolutionary change in function. Perhaps, as stated by Macias and Churchill (2015), this change in behavior causes greater stress on the anterior and posterior aspects of the joint surface, and thus, favors a greater breath of the glenoid fossa. The progressive increase of the width of the glenoid fossa, as well as other aspects of the morphology of the shoulder, could be related to an increase in the capacity to throw objects during the evolution of the genus *Homo*, which has reached its maximum expression in anatomically modern humans (Churchill and Trinkaus, 1990; Churchill and Rhodes, 2009; Roach et al., 2013; Macias and Churchill, 2015). As expected, the glenoid index in ATD6-116 and ATD6-118 is low, following the general trend observed in hominins. If the functional hypothesis is right, then *H. antecessor* would not be a skillful object thrower. Nevertheless, the cause of this adaptive trend remains under discussion (Macias and Churchill, 2015).

Regarding the variability of axillary border morphology Trinkaus (1977) first proposed a functional interpretation. According to this author, this variability could be related to the rotator cuff muscles, which provide stability to the shoulder. In particular, this variability could be associated with a differential hypertrophy of the teres minor muscle in Neanderthals (Trinkaus, 1977). This hypothesis was questioned by Churchill and Trinkaus (1990), who failed to find evidence supporting an inference of hypertrophy of the teres minor muscle in these hominins. Alternatively, they suggested that the variability of the axillary border could be related to bending moments on the scapula. However, this hypothesis has been also questioned by Churchill (1996) and others (Franciscus and Schoenebaum, 2000; Odwak, 2006). These authors failed to find support for a link between the characteristic dorsal sulcus pattern of the Neanderthals with the upper limb robusticity.

From the ontogenetic point of view, it is interesting to ascertain if the different patterns of the axillary border change with age. Some studies concluded that the distinctive ventral or dorsal sulci do not arise prior to 3–5 years after birth (e.g., Kondo and Dodo, 2002; Busby, 2006). However, the presence of the characteristic dorsal sulcus in immature scapulae in some Neanderthals from Krapina and particularly in the Kiik-Koba specimen (probably belonging to a Neanderthal child less than a year old: Vlcek, 1973) suggests that this feature has a genetic basis and is not related to physical activity. In addition, this feature seems to appear very early in ontogeny. The condition in ATD6-116 also supports this view. Furthermore, in the absence of solid evidence to support a functional explanation for axillary variation, morphological differences among species may reflect taxonomic differences and phylogenetic history. According to the evidence of the fossil record, it seems that the ventral sulcus pattern is the plesiomorphic condition for the hominin clade (Trinkaus, 2008), whereas the dorsal sulcus pattern emerged during the Middle Pleistocene in European populations (Carretero et al., 1997). This feature is difficult to identify in anatomically modern humans. Although a substantial percentage of Upper Paleolithic and Mesolithic populations exhibit a dorsal sulcus, this morphology seems to be absent in recent humans, who show both the bisulcate and ventral sulcus (see Table 7 in Carretero et al., 1997).

5. Conclusions

We described and compared two practically complete immature scapulae from the late Early Pleistocene of Europe, obtained at the TD6.2 level of the Gran Dolina cave site of the Sierra de Atapuerca. Our results show that these specimens fill a morphological gap between the scapula of KNM-WT 15000 (1.6 Ma) and the scapulae of the Sima de los Huesos of the Sierra de Atapuerca (0.43 Ma).

With respect to the fossil record, only the DIK-1-1 (*A. afarensis*) and KNM-WT 15000 (*H. erectus/H. ergaster*) specimens exhibit preservation comparable to that of the TD6.2 scapulae. Although KNM-WT 15000 is significantly larger than ATD6-118 the scapular and glenoid indices, as well as the axilloglenoid angle, are similar. Additional comparisons carried out between the TD6.2 scapulae and other fossil specimens, as well as with published data on recent modern humans, allow us to conclude that ATD6-116 and ATD6-118 show the general pattern of the genus *Homo*.

Both ATD6-116 and ATD6-118 exhibit the primitive condition for the hominin clade for the glenoid index and the morphology of the axillary border (sulcus axillaris subscapularis). The presence of the latter in ATD-116 suggests that the shape of the axillary border could have a genetic basis and is not related to physical activity. On the basis of the narrowness of the glenoid fossa, we suggest that *H. antecessor* would not be a skillful object thrower. However, the relationship between glenoid fossa shape and function has been debated, and therefore functional interpretations based on this feature should be approached with caution.

Acknowledgements

Without the effort of the members of the Atapuerca Research Team during fieldwork, this work would have not been possible. We would like to make a special mention to the contribution of Jaume Guiu, who is deeply missed. This report has been mainly supported by the Dirección General de Investigación of the Spanish Ministry of "Ciencia, Innovación y Universidades", grant number PGC2018-093925-B.C31, and the Consejería de Cultura y Turismo of the Junta de Castilla y León, by the British Academy International Partnership and Mobility International Fellowship (PM160019). We also acknowledge The Leakey Foundation through the personal support of Gordon Getty (2013) and Dub Crook (2014, 2015, 2016, 2018) to one of the authors (M.M.-T.), and to the Atapuerca Foundation for their postdoctoral grant to M.M.-P. C.G.-C. and M.M.-M. are funded by a doctoral grant from the European Social Funds (BOCYL-D-30122013-33) through the Consejería de Educación de Castilla y León (Spain). L.M.-F. received financial support from the French State as part of the 'Investments for the future' Programme IdEx Bordeaux, reference code ANR-10-IDEX-03-02. L.L.-P. work is funded by CERCA Programme/Generalitat de Catalunya. The μCT images were obtained in the Laboratory of Microscopy of the CENIEH-Instalación Cientifico Técnica Singular (ICTS) (Spain) in collaboration with CENIEH staff. Some of the figures were prepared by Susana Sarmiento. We sincerely appreciate the generosity and altruism of all those who have participated in the revision of the manuscript.

Appendix A. Supplementary Online Material

Supplementary online material related to this article can be found online at https://doi.org/10.1016/j.jhevol.2019.102689.

References

Alemseged, Z., Spoor, F., Kimbel, W.H., Bobe, R., Geraads, D., Reed, D., Wynn, J.G., 2006. A juvenile early hominin skeleton from Dikika, Ethiopia. Nature 443, 296–301.

Álvarez-Posada, C., Parés, J.M., Cuenca-Bescós, G., Made van der, J., Rosell, J., Bermúdez de Castro, J.M., Carbonell, E., 2018. A post-Jaramillo age for the artefact-bearing layer TD4 (Gran Dolina, Atapuerca): new paleomagnetic evidence. Quaternary Geochronology 45, 1–8.

Arnold, L.J., Demuro, M., Parés, J.M., Pérez-González, A., Arsuaga, J.L., Bermúdez de Castro, J.M., Carbonell, E., 2014. Evaluating the suitability of extended-range luminescence dating techniques over early and Middle Pleistocene timescales: published datasets and case studies from Atapuerca, Spain. Quaternary International 389, 167–190.

Arnold, L.J., Demuro, M., 2015. Insights into TT-OSL signal stability from single-grain analyses of known-age deposits at Atapuerca, Spain. Quaternary Geochronology 30, 472–478.

Badr El Dine, F.M.M., Hassan, H.H.M., 2016. Ontogenetic study of the scapula among some Egyptians: forensic implications in age and sex estimation using multi-detector computed tomography. Egyptian Journal of Forensic Sciences 6, 56–77.

Berger, G.W., Pérez-González, A., Carbonell, E., Arsuaga, J.L., Bermúdez de Castro, J.M., Ku, T.L., 2008. Luminescence chronology of cave sediments at the Atapuerca paleoanthropological site, Spain. Journal of Human Evolution 55, 300–311.

Berger, L.R., de Ruiter, D.J., Churchill, S.E., Schmid, P., Carlson, K.J., Dirks, P.H.G.M., Kibii, J.M., 2010. *Australopithecus sediba*: a new species of *Homo*-like Australopith from South Africa. Science 328, 195–204.

Bermúdez de Castro, J.M., Pérez-González, A., Martinón-Torres, M., Gómez-Robles, A., Rosell, J., Prado, L., Sarmiento, S., Carbonell, E., 2008. A new Early Pleistocene hominin mandible from Atapuerca-TD6, Spain. Journal of Human Evolution 55, 729–735.

Bermúdez de Castro, J.M., Martinón-Torres, M., Martín-Francés, L., Modesto, M., Martínez de Pinillos, M., García, C., Carbonell, E., 2017. *Homo antecessor*. The state of the art eighteen years later. Quaternary International 433, 22–31.

Billy, G., 1975. Étude anthropologique des restes humains de l'Abri Pataud. Bulletin of the American School of Prehistoric Research 30, 201–261.

Brown, F.H., Harris, J., Leakey, R., Walker, A., 1985. Early *Homo erectus* skeleton from west Lake Turkana, Kenya. Nature 316, 788–792.

Busby, A.M., 2006. A multivariate analysis of the ontogeny of the scapular axillary border. Periodicum Biologorum 108, 365–371.

Campaña, I., Pérez-González, A., Benito-Calvo, A., Rosell, J., Blasco, R., Bermúdez de Castro, J.M., Carbonell, E., Arsuaga, J.L., 2016. New interpretation of the Gran Dolina-TD6 bearing *Homo antecessor* deposits through sedimentological analysis. Scientific Reports 6, 34799.

Carbonell, E., Bermúdez de Castro, J.M., Arsuaga, J.L., Díez, J.C., Rosas, A., Cuenca-Bescós, G., Sala, R., Mosquera, M., Rodriguez, X.P., 1995. Lower Pleistocene hominids and artifacts from Atapuerca-TD6 (Spain). Science 269, 826–830.

Carbonell, E., Cáceres, I., Lozano, M., Saladié, P., Rosell, J., Lorenzo, C., Vallverdú, J., Huguet, R., Canals, A., Bermúdez de Castro, J.M., 2010. Cultural cannibalism as a paleoeconomic system in the European Lower Pleistocene. Current Anthropology 51, 539–549.

Carretero, J.M., Arsuaga, J.L., Lorenzo, C., 1997. Clavicles, scapulae and humeri from the Sima de los Huesos site (Sierra de Atapuerca, Spain). Journal of Human Evolution 33, 357–408.

Carretero, J.M., Lorenzo, C., Arsuaga, J.L., 1999. Axial and appendicular skeleton of *Homo antecessor*. Journal of Human Evolution 37, 459–499.

Chhabra, N., Prakash, S., Mishra, B.K., 2015. Morphometric analysis of adult dry human scapulae. International Journal of Medical and Health Research 1, 35–38.

Churchill, S.E., 1994. Human upper body evolution in the Eurasian Latter Pleistocene. Ph.D. Dissertation, University of New Mexico.

Churchill, S.E., 1996. Neandertal scapular axillary border morphology revisited. American Journal of Physical Anthropology Supplement 83, 85.

Churchill, S.E., Rhodes, J.A., 2009. The evolution of the human capacity for "killing at a distance": the human fossil evidence for the evolution of projectile weaponry. In: Hublin, J.-J., Richards, M.P. (Eds.), The Evolution of Hominin Diets: Integrating Approaches to the Study of Paleolithic Subsistence. Springer, Dordrecht, pp. 201–210.

Churchill, S.E., Trinkaus, E., 1990. Neandertal scapular glenoid morphology. American Journal of Physical Anthropology 83, 147–160.

Churchill, S.E., Green, D.J., Feuerriegel, E.M., Macias, M.E., Mathews, S., Carlson, K.J., Schmid, P., Berger, L.R., 2018. The shoulder, and forearm of *Australopithecus sediba*. PaleoAnthropology 2018, 234–281.

Cuenca-Bescós, G., Blain, H.-A., Rofes, J., Lozano-Fernández, I., López-García, J.M., Duval, M., Galán, J., Núñez-Lahuerta, C., 2015. Comparing two different Early Pleistocene microfaunal sequences from the caves of Atapuerca, Sima del Elefante and Gran Dolina (Spain): biochronological implications and significance of the Jaramillo subchron. Quaternary International 389, 148–158.

Dabbs, G.D., Moore-Jansen, P.H., 2010. A method for estimating sex using metric analysis of the scapula. Journal of Forensic Science 55, 149–152.

Dean, C., 2007. Growing up slowly 160,000 years ago. Proceedings of the National Academy of Sciences of the United States of America 104, 6093–6094.

Dean, C., Leakey, M.G., Reid, D., Schrenk, F., Schwartz, G.T., Stringer, C., Walker, A., 2001. Growth processes in teeth distinguish modern humans from *Homo erectus* and earlier hominins. Nature 414, 628–631.

Di Vincenzo, F., Churchill, S.E., Manzi, G., 2012. The Vindija Neanderthal scapular glenoid fossa: comparative shape analysis suggests evo-devo changes among Neanderthals. Journal of Human Evolution 62, 274–285.

Di Vincenzo, F., Churchill, S.E., Buzi, C., Profico, A., Tafuri, M.A., Micheli, M., Caramelli, D., Manzi, G., 2019. Distinct among Neanderthals: the scapula of the skeleton from Altamura, Italy. Quaternary Science Reviews 217, 76–88.

Duval, M., Grün, R., Parés, J.M., Martín-Francés, L., Campaña, I., Rosell, J., Shao, Q., Arsuaga, J.L., Carbonell, E., Bermúdez de Castro, J.M., 2018. The first direct ESR analysis of a hominin tooth from Atapuerca Gran Dolina TD-6 (Spain) supports the antiquity of *Homo antecessor*. Quaternary Geochorology 47, 120–137.
von, Eickstedt, E.F., 1925. Variationen am axillarrand der scapula (sulcus axillaris teretis und sulcus axillaris subscapularis). Anthropolgischer Anzeiger 2, 217–228.
Endo, B., Kimura, T., 1970. Postcranial skeleton of the Amud Man. In: Suzuki, H., Takai, F. (Eds.), The Amud Man and his Cave Site. Academic Press of Japan, Tokyo, pp. 231–406.
Falguères, C., Bahain, J.-J., Yokoyama, Y., Arsuaga, J.L., Bermúdez de Castro, J.M., Carbonell, E., Bischoff, J.L., Dolo, J.-M., 1999. Earliest humans in Europe: the age of Atapuerca fossils, Spain. Journal of Human Evolution 37, 343–352.
Fernández-Jalvo, Y., Díez, J.C., Cáceres, I., Rosell, J., 1999. Human cannibalism in the Early Pleistocene of Europe (Gran Dolina, Sierra de Atapuerca, Burgos, Spain). Journal of Human Evolution 37, 591–622.
Feuerriegel, E.M., Green, D.J., Walker, C.S., Schmid, P., Hawks, J., Berger, L., Churchill, S.E., 2017. The upper limb of *Homo naledi*. Journal of Human Evolution 104, 155–173.
Franciscus, R.G., Schoenebaum, C.R., 2000. Cross-sectional metric analysis of scapular axillary border morphology in recent humans and the Krapina Neandertals. American Journal of Physical Anthropology 30, 152.
Frutos, L.R., 2002. Determination of sex from the clavicle and scapula in a Guatemalan contemporary rural indigenous population. American Journal Forensic Medical Pathology 23, 284–288.
Green, D.J., Alemseged, Z., 2012. *Australopithecus afarensis* scapular ontogeny, function, and the role of climbing in human evolution. Science 338, 514–517.
Green, D.J., Chirchir, H., Mbua, E., Harris, J.W.K., Braun, D.R., Griffin, N.L., Richmond, B.G., 2018. Scapular anatomy of *Paranthropus boisei* from Ileret, Kenya. Journal of Human Evolution 125, 181–192.
Haile-Selassie, Y., Latimer, B.M., Alene, M., Deino, A.L., Gibert, L., Melillo, S.M., Saylor, B.Z., Scott, G.R., Lovejoy, C.O., 2010. An early *Australopithecus afarensis* postcranium from Woranso-Mille, Ethiopia. Proceedings of the National Academy of Sciences of the United States of America 107, 12121–12126.
Johanson, D., Lovejoy, C.O., Kimbel, W.H., White, T.D., Ward, S.C., Bush, M.E., Latimer, B.M., Coppens, Y., 1982. Morphology of the Pliocene partial hominid skeleton (A.L. 288-1) from the Hadar Formation, Ethiopia. American Journal of Physical Anthropology 57, 403–451.
Kondo, O., Dodo, Y., 2002. The postcranial bones of the Neanderthal child of burial n° 1. In: Akazawa, T., Muhesen, S. (Eds.), Neanderthal Burials. Excavations of the Dederiyeh Cace, Afrin, Syria. International Research Center for Japanese Studies, Kyoto, pp. 139–214.
Leakey, R.E.F., Walker, A.C., 1985. Further hominids from the Plio-Pleistocene of Koobi Fora, Kenya. American Journal of Physical Anthropology 67, 135–163.
Lordkipanidze, D., Jahasvili, T., Vekua, A., Ponce de León, M., Zollikofer, C.P.E., Rightmire, G.P., Pontzer, H., Ferring, R., Oms, O., Tappen, M., Bukhsianidze, M., Agusti, J., Kahlke, R., Kiladze, G., Martínez-Navarro, B., Mouskhelishvili, A., Nioradze, M., Rook, L., 2007. Postcranial evidence from early *Homo* from Dmanisi (Georgia). Nature 449, 305–310.
Macias, M.E., Churchill, S.E., 2015. Functional morphology of the Neandertal scapular glenoid fossa. The Anatomical Record 298, 168–179.
Martin, R., 1928. Lehrbuch der Anthropologie, second ed. Fisher Jena.
Melillo, S.M., 2016. The shoulder girdle of KSD-VP-1/1. In: Haile-Selassie, Y., Su, D. (Eds.), The Postcranial Anatomy of *Australopithecus afarensis*. Springer, Netherlands, Dordrecht, pp. 113–141.
Modesto-Mata, M., 2019. Histología dental de los homininos de la sierra de Atapuerca (Burgos, España) y patron de estrategia de vida. PhD. Thesis, Universidad de Burgos, Spain.
Moran, A.J., Chamberlain, A.T., 1977. The incidence of dorsal sulci of the scapula in a modern human population from Ensay, Scotland. Journal of Human Evolution 33, 521–524.
Moreno, D., Falguères, C., Pérez-González, A., Voinchet, P., Ghaleb, B., Despriee, J., Bahain, J.J., Sala, R., Carbonell, E., Bermúdez de Castro, J.M., Arsuaga, J.L., 2015. New radiometric dates on the lowest stratigraphical section (TD1 to TD6) of Gran Dolina site (Atapuerca, Spain). Quaternary Geochronology 30, 535–540.
Mosquera, M., Ollé, A., Rodríguez-Álvarez, X.P., Carbonell, E., 2018. Shedding light on the Early Pleistocene of TD6 (Gran Dolina, Atapuerca, Spain): the technological sequence and occupational inferences. PLOS One 13, e0190889.
Odwak, H., 2006. Scapular axillary border morphology in modern humans and Neandertals. Periodicum Biologorum 108, 353–364.
Parés, J.M., Pérez-González, A., 1995. Paleomagnetic age for hominid fossils at Atapuerca archaeological site, Spain. Science 269, 830–832.
Parés, J.M., Pérez-González, A., 1999. Magnetochronology and stratigraphy at Gran Dolina section, Atapuerca (Burgos, Spain). Journal of Human Evolution 37, 325–342.
Parés, J.M., Sier, M., Duval, M., Woodhead, J., Carbonell, E., Álvarez-Posada, C., Campaña, I., Moreno, D., Ortega, A.I., Bermúdez de Castro, J.M., Rosell, J., 2018. Chronology of the cave interior sediments at Gran Dolina archaeological site, Atapuerca (Spain). Quaternary Science Reviews 186, 1–16.
Rissech, C., Black, S., 2007. Scapular development from neonatal period to skeletal maturity. A preliminary study. International Journal of Osteoarchaeology 17, 451–464.
Roach, N.T., Venkadesan, M., Rainbow, M.J., Lieberman, D.E., 2013. Elastic energy storage in the shoulder and the evolution of high-speed throwing in *Homo*. Nature 498, 483–486.
Robinson, J.T., 1972. Early Hominid Posture and Locomotion. University of Chicago Press, Chicago.
Saladié, P., Huguet, R., Rodríguez-Hidalgo, A., Cáceres, I., Esteban-Nadal, M., Arsuaga, J.L., Bermúdez de Castro, J.M., Carbonell, E., 2012. Intergroup cannibalism in the European Early Pleistocene: the range and imbalance of power hypotheses. Journal of Human Evolution 63, 682–695.
Schaefer, M., Aben, G., Vogelsberg, C., 2015. A demonstration of appearance and union times of three shoulder ossification centers in adolescent and post-adolescent children. Journal of Forensic Radiology and Imaging 3, 49–56.
Scheuer, L., Black, S., 2004. The Juvenile Skeleton. Academic Press/Elsevier, London.
Senut, B., 1981. L'Humerus et ses articulations chez les Hominidés Plio-Pléistocenes. CNRS, Paris.
Smith, B.H., 1993. The physiological age of KNM-WT 15000. In: Walker, A., Leakey, R. (Eds.), The Nariokotome *Homo erectus* Skeleton. Springer-Verlag, Berlin, pp. 195–220.
Trinkaus, E., 1977. A functional interpretation of the axillary border of the Neandertal scapula. Journal of Human Evolution 6, 231–234.
Trinkaus, E., 1983. The Shanidar Neanderthals. Academic Press, New York.
Trinkaus, E., 2006. The Krapina scapulae. Periodicum Biologorum 108, 341–351.
Trinkaus, E., 2008. Kiik-Koba 2 and Neandertal axillary border ontogeny. Anthropological Science 116, 231–236.
Trinkaus, E., Mednikova, M.B., Cowgill, L., 2016. The appendicular remains of the Kiik-Koba 2 Neandertal infant. PaleoAnthropology 2016, 185–2010.
Vallois, H.V., 1928-1946. L'omoplate humaine: Étude anatomique et anthropologique. In: Bulletin et Mémoires de la Societé d'Anthropologie. Paris Série 7, 9, 129-168; 10, 110-191; Série 8, 3, 3-153; Série 9, 7, 16-100.
Vlcek, E., 1973. Postcranial skeleton of a Neandertal child from Kiik-Koba, USSR. Journal of Human Evolution 2, 537–544.
Voisin, J.-L., 2011. A preliminary approach to the Neanderthal speciation by distance hypothesis: a view from the shoulder complex. In: Condemi, S., Weniger, G.-C. (Eds.), Continuity and Discontinuity in the Peopling of Europe, One Hundred Fifty Years of Neanderthal Study. Springer Dordrecht, Heidelberg, London, New York, pp. 127–138.
Vrba, E.S., 1979. A new study of the scapula of *Australopithecus africanus* from Sterkfontein. American Journal of Physical Anthropology 51, 117–130.
Walker, A.C., Zimmerman, M.R., Leakey, R.E.F., 1982. A possible case of hypervitaminosis A in *Homo erectus*. Nature 296, 248–250.
Walker, A.C., Leakey, R.E.F., 1993. The postcranial bones. In: Walker, A., Leakey, R. (Eds.), The Nariokotome *Homo erectus* Skeleton. Springer Verlag, Berlin, pp. 95–160.
Weaver, T.D., 2009. The meaning of Neandertal skeletal morphology. Proceedings of the National Academy of Sciences of the United States of America 106, 16028–16033.